Differential Mobility of Pigment-Protein Complexes in Granal and Agranal Thylakoid Membranes of C_3 and C_4 Plants[1][OA]

Helmut Kirchhoff*, Richard M. Sharpe, Miroslava Herbstova, Robert Yarbrough, and Gerald E. Edwards

Institute of Biological Chemistry (H.K., M.H., R.Y.) and School of Biological Sciences (R.M.S., G.E.E.), Washington State University, Pullman, Washington 99164; and Institute of Plant Molecular Biology, Biology Centre, Academy of Sciences of the Czech Republic, 370 05 Ceske Budejovice, Czech Republic (M.H.)

The photosynthetic performance of plants is crucially dependent on the mobility of the molecular complexes that catalyze the conversion of sunlight to metabolic energy equivalents in the thylakoid membrane network inside chloroplasts. The role of the extensive folding of thylakoid membranes leading to structural differentiation into stacked grana regions and unstacked stroma lamellae for diffusion-based processes of the photosynthetic machinery is poorly understood. This study examines, to our knowledge for the first time, the mobility of photosynthetic pigment-protein complexes in unstacked thylakoid regions in the C_3 plant Arabidopsis (*Arabidopsis thaliana*) and agranal bundle sheath chloroplasts of the C_4 plants sorghum (*Sorghum bicolor*) and maize (*Zea mays*) by the fluorescence recovery after photobleaching technique. In unstacked thylakoid membranes, more than 50% of the protein complexes are mobile, whereas this number drops to about 20% in stacked grana regions. The higher molecular mobility in unstacked thylakoid regions is explained by a lower protein-packing density compared with stacked grana regions. It is postulated that thylakoid membrane stacking to form grana leads to protein crowding that impedes lateral diffusion processes but is required for efficient light harvesting of the modularly organized photosystem II and its light-harvesting antenna system. In contrast, the arrangement of the photosystem I light-harvesting complex I in separate units in unstacked thylakoid membranes does not require dense protein packing, which is advantageous for protein diffusion.

In higher plants, the photosynthetic apparatus is compartmentalized in the specialized chloroplast organelle. The molecular machinery for the primary photosynthetic processes, the sunlight-driven generation of metabolic energy equivalents, is harbored in an intricate thylakoid membrane system within the chloroplasts. Recent improvements in electron tomography have led to three-dimensional models of the complex architecture of thylakoid membranes (Mustárdy and Garab, 2003; Nevo et al., 2009; Austin and Staehelin, 2011; Daum et al., 2010; Kouřil et al., 2011). Although important details about the thylakoid structure are still highly controversial, consensus exists about the overall design of this membrane system. The thylakoid membrane consists of two morphologically distinct domains: strictly stacked cylindrical grana regions with a diameter of 300 to 600 nm are interconnected by unstacked stroma lamellae, thus forming a continuous membrane system. The molecular complexes that catalyze energy transformation are distributed heterogeneously between the stacked and unstacked membrane regions. The majority of the PSII complex and light-harvesting complex II (LHCII) are localized in stacked thylakoid regions, whereas PSI and the ATP-synthase complex are lacking from stacked grana (Staehelin and van der Staay, 1996; Albertsson, 2001; Dekker and Boekema, 2005). It is assumed that the fifth photosynthetic protein complex (cytochrome b_6f complex) is homogenously distributed.

An essential feature of the thylakoid membrane system is its high flexibility, which is required for adaptability and maintenance of the photosynthetic machinery in plants. Highly responsive to environmental conditions, both the overall thylakoid architecture (e.g. number of grana discs) and the molecular membrane composition can change remarkably to optimize, protect, and maintain the photosynthetic apparatus (Walters, 2005; Anderson et al., 2008; Chuartzman et al., 2008; Dietzel et al., 2008; Betterle et al., 2009; Johnson et al., 2011). The underlying molecular processes require brisk protein traffic between stacked and unstacked thylakoid domains (Kirchhoff, 2008). The role of grana in these transport-based processes is poorly understood.

[1] This work was supported by the National Science Foundation (grant no. MCB–115871 to H.K. and grant no. IBN–0641232 to G.E. and R.M.S.), the U.S.-Israel Binational Agricultural Research and Development Fund (grant no. BARD US–4334–10), the U.S. Department of Agriculture (Agriculture Research Center grant no. WNP00775), Washington State University (to H.K.), and by institutional support RVO:60077344 (to M.H.).

* Corresponding author; e-mail kirchhh@wsu.edu.

The author responsible for distribution of materials integral to the findings presented in this article in accordance with the policy described in the Instructions for Authors (www.plantphysiol.org) is: Helmut Kirchhoff (kirchhh@wsu.edu).

[OA] Open Access articles can be viewed online without a subscription.

www.plantphysiol.org/cgi/doi/10.1104/pp.112.207548

Although photosynthetic energy conversion is possible without grana (Anderson et al., 2008), the fact that stacked thylakoids are ubiquitous in almost all land plants (with the exception of chloroplasts in bundle sheath [BS] cells in some C_4 plants; see below) highlights the evolutionary pressure to preserve this complex structural feature. Recently, the importance of grana formation was highlighted in Arabidopsis (*Arabidopsis thaliana*) mutants that lack the *GRANA-DEFICIENT CHLOROPLAST1* gene; they grow much slower than the wild type and exhibit seed lethargy due to missing grana formation (Cui et al., 2011). The functional advantages of grana formation have been discussed extensively (Trissl and Wilhelm, 1993; Mullineaux, 2005; Anderson et al., 2008). It was hypothesized that grana could (1) increase the thylakoid membrane area, and the pigment concentration, in chloroplasts, (2) avoid energy spillover from PSII to PSI, (3) regulate the balance of energy distribution between PSII and PSI by state transition, and (4) enable transversal exciton energy transfer between adjacent grana discs. Although there are good arguments that these possibilities are important for photosynthetic energy conversion, the basis for the evolutionary development of grana has not been determined (Mullineaux, 2005; Anderson et al., 2008).

A less considered aspect of grana formation is that it leads to a concentration of protein complexes (Murphy, 1986; Kirchhoff, 2008). The membrane area fraction that belongs to integral photosynthetic protein complexes is about 70%, making grana discs one of the most crowded biomembranes (Kirchhoff, 2008). Light harvesting by PSII benefits from a high protein-packing density for two reasons. First, a concentration of PSII and LHCII in grana ensures a high concentration of light-absorbing pigments that increase the probability of capturing sunlight, which is a "dilute" energy source on the molecular scale (Blankenship, 2002). Second, it has been demonstrated that a high protein-packing density in grana thylakoids is required for efficient intermolecular exciton energy transfer between LHCII and PSII (Haferkamp et al., 2010). Macromolecular crowding ensures that weakly interacting LHCII and PSII complexes come in close contact, allowing efficient Förster-type energy transfer.

Besides these advantages, lateral protein traffic is challenged by macromolecular crowding (Mullineaux, 2005; Kirchhoff, 2008). The molecular mobility of proteins in grana thylakoids is reduced by numerous collisions of the diffusing object in the two-dimensional reaction space of the membrane with obstacles, integral membrane proteins, that increase the apparent diffusion path and, consequently, the diffusion time. The strong impairment of a high protein density in grana thylakoids on protein mobility was demonstrated by computer simulations (Tremmel et al., 2003; Kirchhoff et al., 2004) and by diffusion measurement on isolated grana membranes (Kirchhoff et al., 2008) and intact chloroplasts (Goral et al., 2010) using the fluorescence recovery after photobleaching (FRAP) technique. Processes that are expected to be affected by restricted protein mobility are a regulation of energy distributed between PSII and PSI by state transitions (Lemeille and Rochaix, 2010), the repair of photodamaged PSII (Mulo et al., 2008), membrane remodeling triggered by long-term environmental changes (Walters, 2005; Anderson et al., 2008), and the biogenesis of the thylakoid membrane network (Adam et al., 2011). Recently, evidence has accumulated that photoprotective high-energy quenching also requires large-scale diffusion-based structural reorganization within grana thylakoids (Betterle et al., 2009; Johnson et al., 2011).

In contrast to our current understanding of diffusion-based processes in thylakoid membranes, knowledge about the factors that determine the mobility of photosynthetic protein complexes in different thylakoid domains is still fragmentary (Mullineaux, 2008). The protein-packing density is very likely a main element that determines protein mobility (Kirchhoff et al., 2008). However, other factors, like electrostatic interactions between proteins by membrane surface charges (Tremmel et al., 2005) or the size and molecular shape of protein complexes (Tremmel et al., 2003), can contribute significantly. However, data only exist about protein mobility for isolated grana thylakoids (Kirchhoff et al., 2008) and for chloroplasts from the grana-containing C_3 plant Arabidopsis (Goral et al., 2010). The diffusion characteristics of the latter are almost completely determined by granal proteins. Limiting information on protein diffusion exists for stroma lamellae of C_3 plants (Consoli et al., 2005; Vladimirou et al., 2009), and no data are available for agranal thylakoids, which occur in BS cells of some C_4 species.

This study fills this gap in the knowledge base by studying lateral protein diffusion in unstacked thylakoid membranes in BS chloroplasts of two NADP-malate enzyme (ME)-type C_4 species, maize (*Zea mays*) and sorghum (*Sorghum bicolor*), in comparison with the grana-containing mesophyll (M) chloroplasts. The analysis was also complemented by studies on isolated thylakoid subfragments (grana core, grana, and stroma lamellae) from Arabidopsis. The protein mobility was measured by FRAP (Mullineaux and Kirchhoff, 2007), which has been shown to be a straightforward method to analyze protein diffusion in photosynthetic membranes by utilizing natural chlorophyll fluorescence (Kirchhoff et al., 2008; Goral et al., 2010). The comparison with diffusion characteristics in unstacked versus stacked membrane areas highlights the significance of grana formation on the lateral mobility of photosynthetic pigment-protein complexes.

RESULTS

Microscopic, Spectroscopic and Biochemical Characterization of Chloroplasts in Isolated BS Strands and M Protoplasts of Maize and Sorghum

In NADP-ME-type C_4 plants, the BS chloroplasts are deficient in grana while the M chloroplasts have well-

developed grana. The structural integrity of the BS cells was verified by confocal laser-scanning microscopy (CLSM) for maize BS strands (Fig. 1A) and sorghum (data not shown). Higher resolution CLSM micrographs show a lamellar membrane organization in BS chloroplasts of maize and sorghum (Fig. 1, B and C) that confirms an agranal thylakoid organization in these chloroplasts (Laetsch, 1971; Metha et al., 1999). In contrast, CLSM images of grana containing M protoplasts from Arabidopsis (Fig. 1D) and maize and sorghum (data not shown) reveal particulate fluorescence spots of about 400 nm in diameter indicative of grana stacks in these cells.

BS and M protoplast preparations of maize and sorghum were further characterized by room-temperature chlorophyll fluorescence spectra and recorded with the same confocal microscope as used for FRAP (Fig. 2). For comparison, emission spectra of isolated grana core and stroma lamellae of Arabidopsis were measured (Fig. 2). Spectra of isolated grana core discs and stroma lamellae differ mainly in the far-red region. The broad shoulder in the far-red region for stroma lamellae (Fig. 2, dashed lines) is caused by the higher abundance of the PSI-LHCI complex, which has a peak emission around 725 nm and low emission at 680 nm at room temperature (Croce et al., 2000). It should be noted that the emission spectra of isolated stroma lamellae still have a maximum around 680 nm that originates from PSII and LHCII complexes (Krause and Weis, 1991). On first thought, this is surprising, because stroma lamellae have a much higher abundance of PSI relative to PSII (Albertsson, 2001). The dominance of the PSII/LHCII emission in isolated stroma lamellae is explainable by their much higher fluorescence yield compared with PSI-LHCI (Krause and Weis, 1991). However, the far-red emission shoulder can be taken as an indicator of PSI/LHCI, which is enriched in stroma lamellae and absent in grana core regions (Fig. 2).

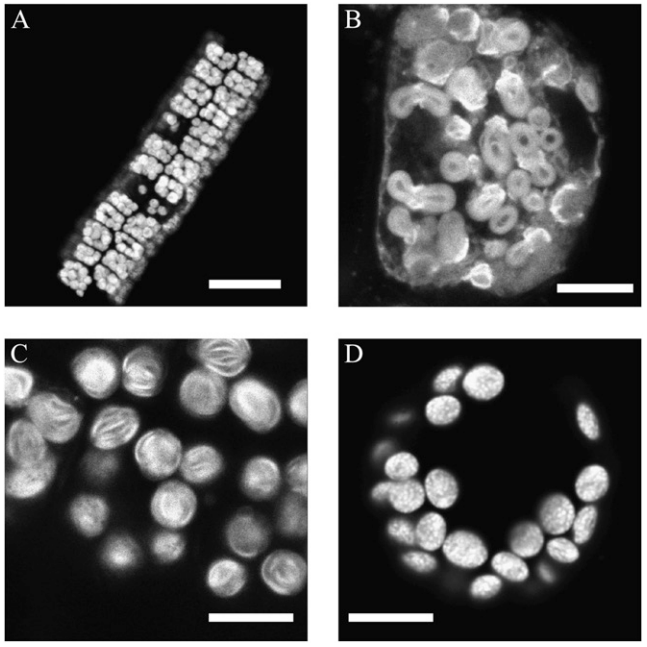

Figure 1. CLSM images of BS strands and M protoplasts of maize and sorghum. The images show natural chlorophyll fluorescence. A, Low-resolution image of an isolated BS strand from maize. B, Closeup CLSM image of a BS cell from maize. C, Chloroplasts within a BS strand of sorghum. D, Chloroplasts within a protoplast isolated from Arabidopsis. Note the small bright spots representing grana discs. Bars = 50 μm (A) and 10 μm (B–D).

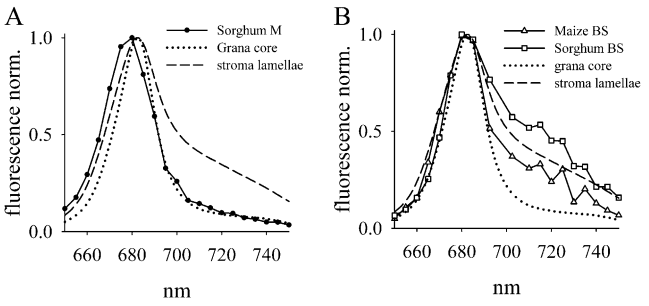

Figure 2. Fluorescence spectra of chloroplasts of M and BS cells from maize and sorghum and of isolated grana core and stroma lamellae from Arabidopsis. Samples were excited at 488 nm. Spectral bandwidth was 10 nm. The spectra for M and BS cell chloroplasts were recorded with similar material to that shown in Figure 1. A, Spectrum of M chloroplasts of sorghum. In addition, spectra of grana core and stroma lamellae of Arabidopsis are shown. Spectra of maize and Arabidopsis M chloroplasts are very similar (data not shown). B, Chlorophyll fluorescence spectra of BS cells from maize and sorghum compared with grana core and stromal lamellae of Arabidopsis.

The fluorescence spectrum for M cells (sorghum is shown as an example in Fig. 2A) is very similar to the isolated grana core of Arabidopsis, indicating the presence of PSII/LHCII-enriched grana. In contrast, the spectra of BS strands from maize and sorghum reveal clear far-red shoulders in accordance with the presence of agranal PSI-LHCI-enriched chloroplasts (Fig. 2B). The higher amplitude of the far-red shoulder relative to the emission around 680 nm in sorghum BS cells is indicative of higher PSI/PSII ratios in sorghum thylakoid membranes compared with their counterparts in maize. For the FRAP measurements presented below, it is important to recognize that the dominance of the 680-nm emission in stroma lamellae and agranal BS chloroplasts implies that mainly PSII/LHCII diffusion was monitored.

The composition of the thylakoid membranes in M and BS cells was characterized by determining their lipid and chlorophyll contents (Table I). The chlorophyll *a*/*b* ratio of maize and sorghum is significantly higher in agranal BS tissues compared with grana-containing M cells, as reported earlier (Ku et al., 1974; Pokorska and Romanowska, 2007). The higher chlorophyll *a*/*b* ratio, and the higher ratios of chlorophyll fluorescence under liquid nitrogen temperature at 730/685 nm for thylakoids of M than for BS thylakoids (5- to 6-fold), are indicative of a much higher abundance of LHCI-PSI complexes in BS thylakoids of

Table I. *Chlorophyll a/b ratios and lipid composition in grana-containing and agranal tissues, and mol % of chloroplast lipids*

Chlorophyll content was determined spectroscopically according to Porra et al. (1989). Lipid content was quantified by two-dimensional TLC. Data represent means with SD from three to six independent measurements.

Sample	Chlorophyll *a*/*b* Ratio	Lipid-Chlorophyll Ratio	MGDG / DGDG / SQDG / PG
		mol mol^{-1}	*mol %*
Arabidopsis leaves	2.8 ± 0.3	1.66 ± 0.12	46 ± 5 / 24 ± 2 / 8 ± 1 / 24 ± 3
Maize M	3.5 ± 0.4	1.51 ± 0.13	45 ± 5 / 36 ± 3 / 14 ± 2 / 5 ± 1
Maize BS	5.7 ± 0.7	3.93 ± 0.19	46 ± 7 / 42 ± 2 / 5 ± 2 / 8 ± 4
Sorghum M	2.9 ± 0.4	2.01 ± 0.17	43 ± 10 / 35 ± 3 / 10 ± 7 / 13 ± 4
Sorghum BS	7.8 ± 2.0	3.36 ± 0.24	44 ± 2 / 37 ± 3 / 7 ± 2 / 12 ± 2

these C_4 plants (Mayne et al., 1974; Romanowska et al., 2008), in agreement with the room-temperature chlorophyll fluorescence spectra (Fig. 2). The lipid composition was measured from total M and BS cells that include extrachloroplast lipids. Information about chloroplast lipids can be extracted from these data by quantification of the three lipid classes, monogalactosyldiacylglycerol (MGDG), digalactosyldiglyceride (DGDG), and sulfoquinovosyl diacylglycerol (SQDG), that are exclusively found in chloroplasts (Benning, 2009). Since more than 80% of the chloroplast lipids are found in thylakoid membranes and less than 20% in envelope membranes (Kirchhoff et al., 2002), the quantification of MGDG, DGDG, and SQDG allows estimation of the lipid content in thylakoid membranes. We also quantified the fourth thylakoid lipid class, phosphatidylglycerol (PG; Table I), that is also found in other cell membranes. Since the ratio of chloroplast to extrachloroplast lipids is high, the contamination with nonchloroplast PG is low. Both the relative abundance of the four lipid classes and the lipid-chlorophyll ratio for Arabidopsis (Table I) are in good agreement with numbers determined for isolated thylakoid membranes from spinach (*Spinacia oleracea*; Kirchhoff et al., 2002). This indicates the validity of the approach to quantify the lipid content for thylakoid membranes from whole-cell lipid extracts.

Since virtually all chlorophylls are bound to membrane-integral photosynthetic protein complexes, the chlorophyll content is a good measure of the protein content in thylakoid membranes. Consequently, the thylakoid lipid-chlorophyll ratio is a good estimate for the protein-packing density in thylakoids (Haferkamp and Kirchhoff, 2008). From the lipid-chlorophyll ratios in Table I, it follows that the protein-packing density in agranal sorghum and maize BS strands is significantly lower (higher lipid-chlorophyll ratio) compared with grana-containing M cells. The impact of these differences in protein packing on the mobility of photosynthetic pigment-protein complexes in thylakoid membranes is reported in the next sections.

FRAP Analysis with BS Strands and M Protoplasts of Maize and Sorghum

For protein diffusion measurements by FRAP, the thylakoid membrane-bound chlorophylls are irreversibly bleached in a small stripe by a short, intense laser excitation (Fig. 3). The time-dependent fluorescence recovery into the bleached line by unbleached pigments from the surrounding area is a direct measure of the diffusion of chlorophyll-protein complexes (e.g. the recovery is fast if the protein mobility is high).

Figure 3 shows FRAP examples for chloroplasts in grana-containing Arabidopsis protoplasts (Fig. 3, A–D) and in agranal sorghum BS chloroplasts (Fig. 3, E–H). For easier comparison, the integrated fluorescence profiles along the *x* axis of the chloroplasts are depicted on the right in each image. The recoveries of the bleach lines (triggered in Fig. 3, B and F) are significantly different in both chloroplast types. After 40 s, the intensity of the stripe is much fainter in sorghum BS chloroplasts (Fig. 3G) than in Arabidopsis (Fig. 3C); after 130 s, the line in Arabidopsis is still visible (Fig. 3D) but that in sorghum BS chloroplasts is not visible, indicating faster recovery (Fig. 3H). This shows that the overall mobility of chlorophyll-protein complexes is higher in the agranal chloroplasts compared with their grana-containing counterparts in Arabidopsis.

Statistical analyses of the fluorescence recovery kinetics of grana-containing and agranal chloroplasts are depicted in Figure 4. Two pieces of information can be extracted from FRAP kinetics: (1) the fraction of mobile molecules (in our case, the chlorophyll-protein complexes) and (2) the diffusion coefficient of the mobile molecules. Reliable determination of the diffusion

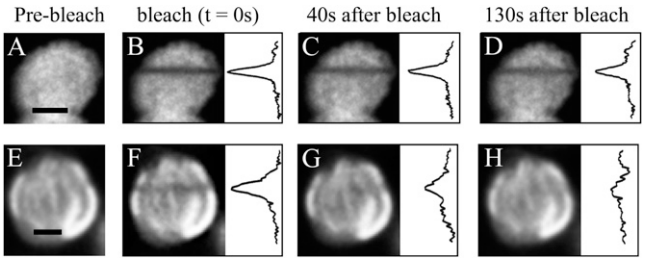

Figure 3. FRAP measurements on Arabidopsis protoplasts (A–D) and sorghum BS cells (E–H). The images show individual chloroplasts before the bleach (A and E), directly after the bleach (B and F), and postbleach images at two different time points (C/G and D/H). For a better comparison between Arabidopsis and sorghum, fluorescence profiles are shown at the right for each bleach image. Bars = 2 μm.

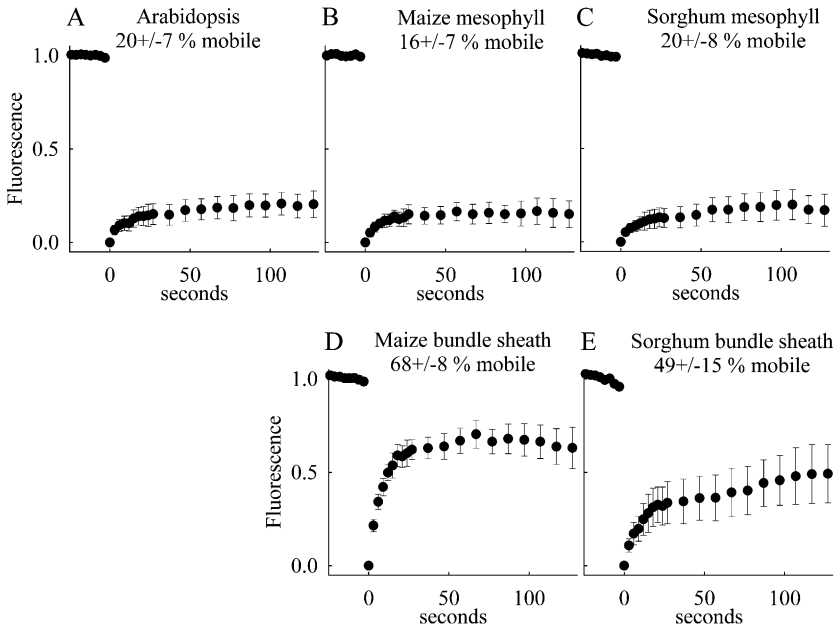

Figure 4. Fluorescence recovery kinetics. From the fluorescence profiles (Fig. 3), the maximum fluorescence intensity for the bleach line is extracted for each time point and plotted versus time. The first image after bleaching was set to 0 s. The fluorescence intensities were normalized to the prebleach values. Data represent mean values with SD from eight to 29 measurements from two preparations. The mobile fractions (with SD) deduced from the fluorescence recovery kinetics are indicated.

coefficient is only possible if the membrane structure is simple (e.g. flat planar membranes; Mullineaux and Kirchhoff 2009). This precondition is not fulfilled for the complex structured thylakoid membrane system examined in this study. However, the mobile fraction can be accurately determined. In Figure 4, this fraction is determined as the ratio of the fluorescence level at the end of the measuring window to the level before the bleach (the fluorescence level directly after the bleach at time zero in Fig. 4 was set to zero). The calculated numbers for the mobile fraction (in percent) are indicated in Figure 4. The analysis clearly shows differential protein mobility in grana-containing M chloroplasts of Arabidopsis, maize, and sorghum (Fig. 4, A–C) and agranal BS tissues of maize and sorghum (Fig. 4, D and E). While the mobile fraction in M cells was between 16% and 20%, this percentage increased to approximately 50% to 70% in agranal BS cells in sorghum and maize, respectively. The value of 20% mobile fraction for the C_3 plant Arabidopsis (Fig. 4A) is in accordance with recently published numbers for isolated chloroplasts (Goral et al., 2010). These data indicate that the formation of grana leads to a decreased mobility of photosynthetic pigment-protein complexes.

Protein Mobility Analysis in Isolated Grana and Stroma Thylakoid Membranes of Arabidopsis

For further characterization of differential protein mobility in stacked and unstacked thylakoid regions, FRAP measurements were performed on isolated stroma lamellae, grana (including grana margins), and grana core subfragments from Arabidopsis plants. In particular, the comparison of the mobile fractions in isolated stroma lamellae with agranal BS cells is interesting, since the protein organization in these unstacked membranes is different (see "Discussion").

The identities of the three membrane domains were verified by their chlorophyll *a*/*b* ratios and by their protein composition as analyzed by denaturative gel electrophoresis (SDS-PAGE; Fig. 5). The chlorophyll *a*/*b* ratios of 4.92 for stroma lamellae, 2.56 for grana, and 2.34 for grana core are in accordance with literature values for these three thylakoid subdomains (Albertsson, 2000). The identity of the three subdomains is further supported by the abundance of α-subunit (approximately 54 kD; *atpA* gene product) and β-subunit (approximately 50 kD; *atpB* gene product) of the CF_1 part of the ATP synthase complex in stroma lamellae and its depletion in grana and grana core as seen on SDS gels (Fig. 5D), since the ATPase complex is excluded from stacked thylakoid regions by steric hindrance (Albertsson, 2001). In addition, densiometric analysis of the *AtpA* and *AtpB* bands reveals that the grana core membranes (16% *AtpA* and 14% *AtpB* abundance relative to thylakoids) are more depleted in these subunits than in grana preparations (24% and 27%). This indicates that the grana, compared with the grana core, contains a higher amount of ATPase-containing grana margins (Albertsson, 2001), which is in line with the higher chlorophyll *a*/*b* ratio (Fig. 5). Finally, the depletion of the 25-kD band in stroma lamellae is indicative of a low abundance of LHCII, as expected for this thylakoid domain (Bassi et al., 1995).

FRAP studies on the three thylakoid subdomains show the highest mobile fraction in stroma lamellae. The value of about 55% is in the range found for agranal BS cells (Fig. 4). In contrast, the mobile fraction in grana and grana core preparations is much lower, with the lowest values logged for grana core membranes. The recorded difference between the two

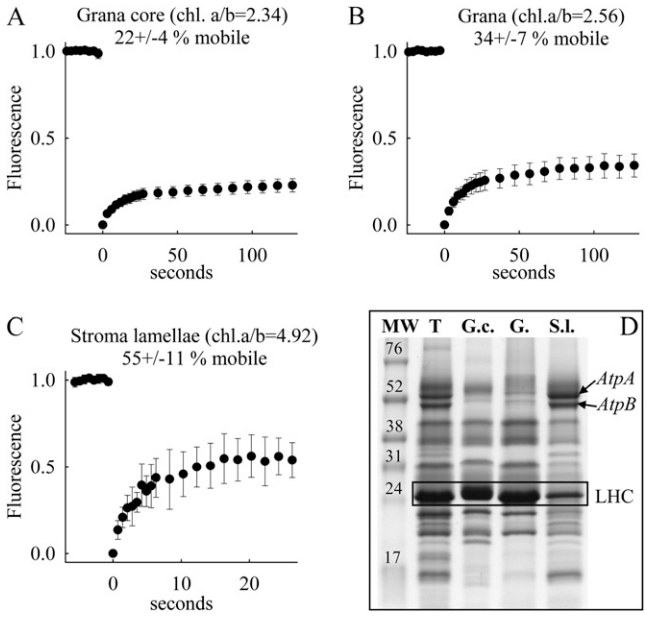

Figure 5. A to C, Fluorescence recovery kinetics for grana core (A), grana including margins (B), and stroma lamellae (C) isolated from Arabidopsis. The data shown represent mean values with SD of 14 to 19 measurements collected from one preparation. D, SDS-PAGE analysis showing protein composition of the thylakoids (T), grana core (G.c.), grana (G.), and stroma lamellae (S.l.) preparations. An amount of sample corresponding to 5 μg of chlorophyll per lane was loaded into each well. Apparent molecular weights were estimated by coelectrophoresis of a low-molecular-weight protein standard (MW; Invitrogen). Bands for the ATPase subunits (*AtpA* and *AtpB* protein) as an indicator of unstacked stroma lamellae are depicted. In addition, the LHCII band is boxed as an indicator of stacked grana.

grana preparations is statistically significant (Student's *t* test, $P = 0.010$). This indicates that the additional margin contribution in grana increases the overall protein mobility.

DISCUSSION

Chloroplasts in plants generally consist of grana and stromal lamellae, which are remarkably different in composition, with primary functions of PSII in grana and PSI and ATP synthase in the stromal lamellae. Besides functioning cooperatively with PSII in the grana in linear electron flow for generating NADPH, PSI may function independently in the stroma lamellae in PSI-mediated cyclic photophosphorylation (Johnson, 2011). An unusual type of chloroplast exists in BS chloroplasts of NADP-ME-type C_4 species, which, like the stromal lamellae, are deficient in grana and PSII but rich in PSI. The primary function of BS chloroplasts is the generation of ATP, while the M chloroplasts have a major role in providing reductive power for CO_2 assimilation (Edwards and Walker, 1983; Hatch, 1987). Among the NADP-ME monocots, sorghum and sugarcane (*Saccharum officinarum*) have extreme deficiency, with agranal BS chloroplasts and PSII activity less than 1% of that of M cell chloroplasts, and maize has a few rudimentary grana in BS chloroplasts, with PSII activity approximately 3% of that of M cell chloroplasts (Laetsch, 1971; Ku et al., 1974). PSII activity was measured with *p*-benzoquinone as a Hill oxidant with intact isolated M protoplasts and BS strands. Low levels of PSII in the BS chloroplasts may provide redox poise for PSI-dependent cyclic photophosphorylation to compensate for electrons lost from the cycle (Ivanov et al., 2007; Romanowska et al., 2008). Thus, the unstacked thylakoid membranes of BS chloroplasts of these species provide a good model for studying protein diffusion in relation to composition and function of the stromal lamellae in chloroplasts having grana.

In chloroplasts of C_3 plants, not only are the types of protein complexes and supercomplexes different between grana and stromal lamellae (Albertsson, 2001), there is also a difference in the protein-packing density. Both the biochemical data (Murphy, 1986) as well as ultrastructural data (Staehelin and van der Staay, 1996) indicate that stroma lamellae in C_3 plants are significantly less crowded by membrane integral proteins than are grana membranes. In this study, the comparison of FRAP data of grana core, grana (with margins), and stroma lamellae in Arabidopsis, a C_3 plant (Fig. 5), revealed that the lower protein-packing densities in grana margins and, in particular, in stroma lamellae correspond to higher protein mobility. The same pattern was observed between agranal BS cells and grana-containing M cell thylakoids from the C_4 plants maize and sorghum (Fig. 4; i.e. BS cells have a lower protein-packing density and higher mobile fractions in thylakoid membranes than M cells). Two conclusions can be drawn from these data. First, grana formation leads to tighter packing of membrane-embedded protein complexes. In this respect, the significantly lower protein-packing density in agranal BS chloroplasts, as determined in this study, complements the existing data on stroma lamellae in C_3 chloroplasts (Murphy, 1986; Staehelin and van der Staay, 1996). Second, higher protein-packing density in grana thylakoids decreases the mobility of grana-hosted proteins. This is in agreement with in vitro studies on isolated grana membranes (Berthold, Babcock, and Yocum [BBY] membranes) with different lipid-protein ratios, which show a strong dependency of the immobile fraction in FRAP experiments on protein density (Kirchhoff et al., 2008). The protein mobility data on agranal and grana-containing chloroplasts in different cells is summarized in Figure 6. To verify that the lipid-chlorophyll ratio (Fig. 6A) is an adequate measure for protein density in the different thylakoid types, we compared the mobile fraction with the lipid-protein ratio in washed thylakoids (Fig. 6B). Washing with the chaotropic sodium thiocyanate (NaSCN) removes extrinsic and attached proteins to thylakoid membranes (Fiedler et al., 1994). Thus, protein determination after NaSCN treatment specifically measures only membrane

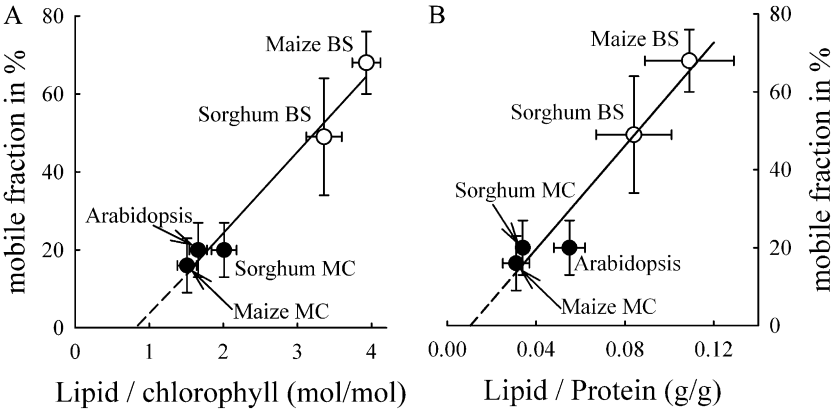

Figure 6. Dependency of the mobile fraction determined from FRAP measurements on the lipid-chlorophyll ratio (A) or the lipid-protein ratio (B). Data represent means with SD. Further statistical information for the mobile fraction is given in Figure 4 and for the lipid-chlorophyll data in Table I. The lipid-protein ratio data were collected from two to four independent measurements. The regression line for A is $y = -17.3 + 20.8x$ (r^2 = 0.973). For B, the regression equation is $y = -6.9 + 663.1x$ (r^2 = 0.973). MC, M cell.

integral complexes. Since both the lipid-chlorophyll (Fig. 6A) and lipid-protein (Fig. 6B) ratios correlate linearly with the mobile fraction, the lipid-chlorophyll ratio provides a measure of the relative protein density in the examined thylakoid membranes. For comparison with literature data, we focus on the lipid-chlorophyll ratio (Fig. 6A) in the further discussion. The good linear correlation (r^2 = 0.973) between the mobile fraction and the lipid-chlorophyll ratio for the different species having different thylakoid architectures (Fig. 6A) give strong evidence that the dependency of protein mobility on protein density is a general principle realized in higher plant thylakoid membranes. This is supported by the fact that protein mobility in isolated stroma lamellae from Arabidopsis is similar to the mobility in agranal BS cells. Both have a lower protein density compared with grana thylakoids and have PSI, cytochrome b_6f complexes, and ATP synthase with low levels of PSII reaction centers. However, it was recently shown that agranal BS cells of maize contain dimeric LHCII/PSII supercomplexes (Romanowska et al., 2008), whereas the stromal lamellae of C_3 plants have monomeric PSII complexes (Danielsson et al., 2006). This indicates that the packing density of membrane complexes determines their mobility, rather than any difference in PSII centers. This does not exclude the possibility that protein mobility can be modulated by other factors like electrostatic effects and/or by the different shapes or sizes of the proteins. Rather, it highlights the dominant role of protein-packing density.

From extrapolation of the regression line in Figure 6A, the lipid-chlorophyll ratio where all proteins are immobile (intersection with the x axis) and where all proteins are mobile (at 100% mobility) can be predicted. It follows that at a molar lipid-chlorophyll ratio of approximately 0.8, all proteins in thylakoid membranes are expected to be immobile. It is interesting to compare this value with the number 1.13 (Kirchhoff et al., 2002), which is the required lipid-chlorophyll ratio needed to encircle all thylakoid protein complexes with one layer of lipids (so-called boundary lipids). This comparison indicates that at a lipid-chlorophyll ratio of approximately 0.8, not enough lipids are available to avoid direct protein-protein contact between photosynthetic supercomplexes, and in consequence, all proteins are immobilized in thylakoid membranes. This may be realized by a homogenous depletion of boundary lipids between all protein complexes or a by heterogeneous depletion (i.e. many proteins are in direct contact, creating free lipid space in other membrane areas). However, a critical lowest lipid amount in thylakoid membranes is obviously required to ensure minimal flexibility of the protein network, which is required to adjust and maintain the photosynthetic machinery (see the introduction). How the lipid-protein ratio is adjusted in photosynthetic membranes remains an important point for future research.

The other extreme deduced from Figure 6A is the lipid-chlorophyll ratio where all proteins are mobile. This is expected at approximately six lipids per chlorophyll, in accordance with the protein-density titration experiment with isolated grana (BBY) membranes (Kirchhoff et al., 2008). In the BBY study, the highest level of mobile proteins was found at a lipid-chlorophyll ratio of approximately 7. The original number of 10 added lipids per chlorophyll was corrected to the measured lipid-chlorophyll ratio in the final preparation (Haferkamp and Kirchhoff, 2008), as this is equivalent to what is used in our study. Furthermore, at a threshold value of approximately six lipids per chlorophyll (corrected as above), maximal functional uncoupling between LHCII and PSII in BBY membranes is reached (Haferkamp et al., 2010). This functional uncoupling was explained by protein dilution-induced separation of weakly interacting LHCII and PSII supercomplexes, leading to the disruption of Förster-type exciton energy transfer. In this context, it is interesting that a significant fraction of functional uncoupled LHCII was detected in BS cells of maize (Romanowska et al., 2008). In light of our findings, this can be explained by the lower protein-packing density in BS thylakoid membranes, which leads to the separation and functional uncoupling of LHCII from PSII.

This study demonstrates that the lower protein-packing density in unstacked thylakoid membrane regions facilitates lateral protein mobility. In turn,

concentrating proteins by grana formation impairs efficient protein transport. An example where this differential mobility could be relevant is the PSII repair cycle that reactivates photodamaged PSII (Tikkanen and Aro, 2012). In C_3 plants, PSII is photodamaged in stacked grana regions, whereas the main components of its repair machinery are localized in unstacked stroma lamellae (Tikkanen and Aro, 2012). Thus, repair of PSII depends on lateral protein traffic between grana thylakoids and stroma lamellae. Evidently, this structural separation is not present in agranal BS cells of C_4 plants. Interestingly, the degradation of photodamaged PSII in maize is significantly faster in agranal BS chloroplasts than in M cells (Pokorska and Romanowska, 2007). This could be due to faster migration of damaged components of PSII in agranal membranes. It follows that the formation of stacked grana could lead to a kinetic restriction of the PSII repair cycle in granal thylakoids of C_3 chloroplasts and M chloroplasts of C_4 plants. Our Monte Carlo computer simulations predicted that the PSII supercomplex localized in grana discs required about 1 h to reach the unstacked stroma lamellae (Kirchhoff et al., 2004). The situation in native membranes of C_3 plants is more complex than in the computer simulations. For example, phosphorylation of damaged PSII subunits causes a slight overall increase in protein mobility (Goral et al., 2010; Herbstová et al., 2012) and disassembly of the supercomplex (Pesaresi et al., 2011; Tikkanen and Aro, 2012). Both could speed up lateral diffusion of damaged PSII out of the grana. However, the observation of faster PSII degradation in agranal BS thylakoids of a C_4 plant points to a significant contribution of lateral protein diffusion for PSII repair in grana-containing thylakoid membranes.

An open question remains why the protein-packing densities of stacked and unstacked thylakoid subdomains are different. A possible explanation is that the different light-harvesting antenna organizations of PSII and PSI play an important role. In higher plants, PSI occurs as individual units that bind up to four or five LHCI (Busch and Hippler, 2011). In contrast, the organization of PSII and LHCII in stacked grana is more complex. The structural and functional PSII building block is a dimeric supercomplex that includes two strongly bound LHCII trimers. In addition, up to six more loosely bound LHCII are connected to the supercomplex (Anderson, 1986; Kirchhoff et al., 2007). Furthermore, on the supramolecular level, PSII and LHCII complexes form a connected light-harvesting network manifested by an exchange of excitonic energy between several PSII centers (Joliot and Joliot, 1964; Kramer et al., 2004), a phenomenon called connectivity. Recently, we demonstrated that this functional interaction in grana between numerous protein complexes requires a tight interaction between PSII supercomplexes and LHCII (Haferkamp et al., 2010). This is accomplished by high packing density in grana discs. Thus, macromolecular crowding is a prerequisite for efficient conversion of sunlight by PSII and its antenna system. On the contrary, the light-harvesting interaction with PSI in unstacked stroma lamellae does not require intermolecular energy transfer between different LHCI-PSI supercomplexes. Therefore, the protein-packing density can be lower. As shown in this study, this is an advantage for lateral protein traffic. Since BS thylakoids in NADP-ME-type C_4 plants are optimized to produce mainly ATP by cyclic electron transport, and they are depleted in PSII but enriched in PSI, their thylakoid membranes have a protein-packing density similar to stroma lamellae, which consequently allows for higher protein mobility.

CONCLUSION

Grana formation leads to a macromolecular crowding that is required for efficient light harvesting by the modularly organized PSII/LHCII system. Optimizing this function seems to be a higher evolutionary priority than allowing a high mobility of grana-hosted protein complexes. It is important to note that although 70% to 80% of the protein complexes in grana are virtually immobile, the remaining protein complexes are very mobile (Kirchhoff et al., 2008). It is likely that the mobile fraction increases under environmental conditions that require brisk lateral protein transport through the crowded grana (Herbstová et al., 2012). In unstacked thylakoid membranes, the need to pack protein complexes tightly is not required because of the nonmodular organization of the PSI/LHCI system. Thus, the physicochemical forces that govern tight protein packing in grana stacks are not operative in unstacked regions, leading to a lower protein-packing density and higher protein mobility. Obviously, high protein-packing densities are only formed if required (e.g. for efficient light harvesting), but high packing densities do not occur if not needed, due to interference in the mobility of membrane constituents.

MATERIALS AND METHODS

M Protoplast and BS Preparations

Maize (*Zea mays*) inbred T43 and sorghum (*Sorghum bicolor*) leaves were harvested from 1-month-old plants grown in computer-controlled growth chambers (Econair GC-16; Bio Chambers) under a 14-h-light/10-h-dark photoperiod and a 32°C/18°C temperature regime. A maximum of 900 μmol quanta m^{-2} s^{-1} photosynthetic photon flux density (PPFD) at the midday light period was obtained in a stepwise manner by regulating the lights in 2-h increments. Arabidopsis (*Arabidopsis thaliana* ecotype Columbia) plants were grown in the same type of chamber, with a midday maximum of 400 μmol quanta m^{-2} s^{-1} PPFD, a 12-h/12-h light/dark photoperiod, and day/night temperature of 25°C/18°C. Mature leaves were harvested from 1-month-old plants.

BS strands were isolated mechanically and M protoplasts were isolated enzymatically from maize and sorghum, following a process similar to that described by Sheen (1995) and modified by Markelz et al. (2003) and Sharpe et al. (2011). For the preparation of BS strands, the eighth emergent leaf was divided into five equal sectors; the distal fourth sector was sampled and cut into 2-mm square segments. Segments were submerged in BS buffer I (0.33 M sorbitol, 0.3 M NaCl, 0.001 M EDTA, 0.001 M dithiothreitol, and 0.2 M Tris [pH 9.0]) and processed with several 10-s pulses in a Polytron blender. BS strands were collected via filtration through a 60-μm mesh and then reprocessed with

30-s pulses in a Polytron blender with BS buffer II (0.35 M sorbitol, 0.005 M EDTA, 0.1% [v/v] β-mercaptoethanol, and 0.05 M Tris [pH 8.0]). BS strands were refiltered and microscopically observed. Processing by blending in BS buffer II was repeated until BS strands, free of all attached M cells, were collected. M protoplasts were prepared from leaf samples of maize and sorghum (the fourth sector as described above) and from mature leaves of Arabidopsis. Transverse sections (1–2 mm) were prepared and incubated in enzymatic digestion medium including 5 mM MES-NaOH, pH 5.8, 10 mM $CaCl_2$, 0.6 M sorbitol, 2% (w/v) Sumizyme C (Shin-Nihon Chemical), and 0.1% Macerase (Calbiochem) and gently rocked on a shaker for 2.5 to 3 h. At the end of the incubation, M protoplasts were filtered from the tissue strips using a 60-μm mesh. Protoplasts were pelleted at 15*g* for 5 min, washed once with 5 mM MES-NaOH, pH 5.8, 10 mM $CaCl_2$, and 0.6 M sorbitol, repelleted, and resuspended in the same medium.

Membrane Preparations

Arabidopsis plants were grown in soil under short-day conditions (9 h of light/15 h of dark) with 100 μmol quanta m^{-2} s^{-1} PPFD at a constant temperature of 20°C in a growth chamber. Leaves of 4- to 6-week-old plants were harvested at the end of the dark period, and isolation procedures were carried out in darkness under dim green light in a cold room. Washed leaves were briefly ground in a blender (3–10 s) with ice-cold medium containing 50 mM HEPES (pH 7.5), 0.33 M sorbitol, 1 mM EDTA, 15 mM NaCl, 5 mM $MgCl_2$, 5 mM $CaCl_2$, 0.15% (w/v) bovine serum albumin, and 1 mM sodium ascorbate. The homogenate was immediately filtered through four layers of cotton gauze and one layer of Miracloth and centrifuged for 5 min at 3,200*g*. The chloroplast pellet was suspended with a brush in a hypotonic medium containing 50 mM HEPES (pH 7.5), 15 mM NaCl, and 10 mM $MgCl_2$ and allowed to stand for 10 min in the dark on ice in order to lyse chloroplasts. To remove unbroken material, the solution was shortly centrifuged for 1 min at 200*g*. The supernatant was then subjected to subsequent centrifugation for 10 min at 3,200*g* to pellet thylakoid membranes, which were suspended in a storage buffer containing 50 mM HEPES (pH 7.5) 0.1 M sorbitol, 15 mM NaCl, and 10 mM $MgCl_2$. Thylakoids were subfractionated into grana and stroma lamellae by digitonin treatment followed by differential centrifugations as described by Fristedt et al. (2009). Grana core membranes were isolated by mechanical fractionation of isolated thylakoids followed by aqueous two-phase partition according to Svensson and Albertsson (1989).

Lipid Analysis

BS strands or protoplasts from maize, sorghum, or Arabidopsis leaves were ground in liquid nitrogen. The organic components were extracted with chloroform:methanol (2:1, v/v) and separated from aqueous components by a two-phase system established by the addition of 1 M KCl solution. The green organic phase was harvested, dried completely with nitrogen gas, and dissolved in chloroform (lipid extract). Lipids were separated by two-dimensional thin-layer chromatography (TLC) and stained by bathing the TLC plates in 10% copper sulfate and 7.5% phosphoric acid, followed by heating at 170°C as described by Haferkamp and Kirchhoff (2008). The four types of thylakoid lipids were quantified by comparing their staining intensity with the staining of reference lipid (Lipid Products; Haferkamp and Kirchhoff, 2008). The chlorophyll concentration of the lipid extract was determined spectroscopically according to Porra et al. (1989), and the lipid-to-chlorophyll ratio was calculated.

Protein Analysis

BS strands or M protoplasts from maize, sorghum, or Arabidopsis leaves were homogenized in a protoplast buffer (without enzymes) with a Brinkman homogenizer and then ground in liquid nitrogen. The extract was pottered for 12 plunges and then filtered through an 80-μm mesh followed by a 20-μm mesh. The eluate was centrifuged at maximum speed (25,000*g*) with an Eppendorf 5417R table centrifuge. The pellet was then resuspended in distilled water and subjected to a membrane pretreatment (exposure to 5 M NaSCN to bind extrinsic proteins) according to Fiedler et al. (1994). Protein concentration was then determined using a standard Lowry assay via Folin-Ciocalteu reagent. We determined that the lipid-protein ratio increases with increasing amounts of membranes used for protein determination. Therefore, all protein determinations were performed at chlorophyll concentrations between 100 and 150 μg mL^{-1}. In this concentration range, the lipid-chlorophyll ratio levels off.

Gel Electrophoresis

Protein composition was determined by SDS-PAGE on 12.5% polyacrylamide gels (Laemmli, 1970) containing 6 M urea using Coomassie blue staining.

FRAP Measurements

M protoplast or BS samples were directly placed on a glass slide and covered with a coverslip. For measurements with isolated grana core, grana, and stroma lamellae of Arabidopsis, the glass slide was covered with a bilayer of phosphatidylcholine to avoid artificial glass-membrane interactions (Kirchhoff et al., 2008). For isolated stroma lamellae, the mobile fraction with and without the phosphatidylcholine support system was 55% and 33.5%, respectively. This indicates that the glass-membrane interactions impede protein mobility, and it highlights the importance of using a fluid support system to analyze protein mobility in isolated membranes. Furthermore, the measurements with isolated thylakoid subdomains were performed under anaerobic conditions (Kirchhoff et al., 2008). For fluorescence spectra and FRAP experiments, a Leica SP5 confocal laser-scanning microscope with an Acousto-Optical Beam Splitter system was used. Chlorophyll fluorescence was excited at 488 nm (argon line) and detected between 650 and 720 nm. The FRAP series includes eight prebleaches, the bleach, 10 postbleaches with 3-s separation, and 10 postbleaches with 10-s separation.

A critical assumption for the application of FRAP is the irreversibility of the bleached pigments (i.e. the recovery should be dependent on the diffusion of unbleached pigments from neighboring regions into the bleached stripe only). We verified this by bleaching whole chloroplasts or whole subthylakoid patches. The recovery of these totally bleached samples is very low. The data presented in Figures 4 and 5 are corrected against the total bleach recovery.

Mathematical Analysis

FRAP images were analyzed with ImagePro and SigmaPlot (version 11) software. From the CLSM time series, one-dimensional fluorescence profiles were extracted from each image by summing the fluorescence in the *x* direction (Fig. 3). Because the sample size is small, bleaching results in a significant decrease in the total fluorescence from the sample (FRAP analysis assumes an infinite reservoir of unbleached pigments). To correct for this, the profiles were normalized to the same total fluorescence of each image. The prebleach fluorescence profile was then subtracted from the postbleach fluorescence profiles to generate differential bleach profiles. From these bleach profiles, the maximum level was plotted versus time (Figs. 4 and 5). The mobile fraction was estimated by comparing the first postbleach profile with the profiles obtained at the longest time points.

Received September 21, 2012; accepted November 10, 2012; published November 12, 2012.

LITERATURE CITED

Adam Z, Charuvi D, Tsabari O, Knopf RR, Reich Z (2011) Biogenesis of thylakoid networks in angiosperms: knowns and unknowns. Plant Mol Biol **76:** 221–234

Albertsson P-A (2000) The domain structure and function of the thylakoid membrane. Recent Res Dev Bioenerg **1:** 143–171

Albertsson P-A (2001) A quantitative model of the domain structure of the photosynthetic membrane. Trends Plant Sci **6:** 349–358

Anderson JM (1986) Photoregulation of the composition, function, and structure of thylakoid membranes. Annu Rev Plant Physiol **37:** 93–136

Anderson JM, Chow WS, De Las Rivas J (2008) Dynamic flexibility in the structure and function of photosystem II in higher plant thylakoid membranes: the grana enigma. Photosynth Res **98:** 575–587

Austin JR II, Staehelin LA (2011) Three-dimensional architecture of grana and stroma thylakoids of higher plants as determined by electron tomography. Plant Physiol **155:** 1601–1611

Bassi R, Marquardt J, Lavergne J (1995) Biochemical and functional properties of photosystem II in agranal membranes from maize mesophyll and bundle sheath chloroplasts. Eur J Biochem **233:** 709–719

Benning C (2009) Mechanisms of lipid transport involved in organelle biogenesis in plant cells. Annu Rev Cell Dev Biol **25:** 71–91

Betterle N, Ballottari M, Zorzan S, de Bianchi S, Cazzaniga S, Dall'osto L, Morosinotto T, Bassi R (2009) Light-induced dissociation of an antenna

hetero-oligomer is needed for non-photochemical quenching induction. J Biol Chem **284:** 15255–15266

Blankenship RE (2002) Molecular Mechanisms of Photosynthesis. Blackwell Science, London

Busch A, Hippler M (2011) The structure and function of eukaryotic photosystem I. Biochim Biophys Acta **1807:** 864–877

Chuartzman SG, Nevo R, Shimoni E, Charuvi D, Kiss V, Ohad I, Brumfeld V, Reich Z (2008) Thylakoid membrane remodeling during state transitions in *Arabidopsis*. Plant Cell **20:** 1029–1039

Consoli E, Croce R, Dunlap DD, Finzi L (2005) Diffusion of light-harvesting complex II in the thylakoid membranes. EMBO Rep **6:** 782–786

Croce R, Dorra D, Holzwarth AR, Jennings RC (2000) Fluorescence decay and spectral evolution in intact photosystem I of higher plants. Biochemistry **39:** 6341–6348

Cui Y-L, Jia Q-S, Yin Q-Q, Lin G-N, Kong M-M, Yang Z-N (2011) The *GDC1* gene encodes a novel ankyrin domain-containing protein that is essential for grana formation in Arabidopsis. Plant Physiol **155:** 130–141

Danielsson R, Suorsa M, Paakkarinen V, Albertsson P-A, Styring S, Aro E-M, Mamedov F (2006) Dimeric and monomeric organization of photosystem II: distribution of five distinct complexes in the different domains of the thylakoid membrane. J Biol Chem **281:** 14241–14249

Daum B, Nicastro D, Austin J II, McIntosh JR, Kühlbrandt W (2010) Arrangement of photosystem II and ATP synthase in chloroplast membranes of spinach and pea. Plant Cell **22:** 1299–1312

Dekker JP, Boekema EJ (2005) Supramolecular organization of thylakoid membrane proteins in green plants. Biochim Biophys Acta **1706:** 12–39

Dietzel L, Bräutigam K, Pfannschmidt T (2008) Photosynthetic acclimation: state transitions and adjustment of photosystem stoichiometry. Functional relationships between short-term and long-term light quality acclimation in plants. FEBS J **275:** 1080–1088

Edwards GE, Walker DA (1983) C_3, C_4: Mechanisms, and Cellular and Environmental Regulation, of Photosynthesis. Blackwell Scientific Publications, Oxford

Fiedler HR, Ponomarenko S, von Gehlen N, Strotmann H (1994) Proton gradient-induced changes of the interaction between CF_0 and CF_1 as probed by cleavage with NaSCN. Biochim Biophys Acta **1188:** 29–34

Fristedt R, Willig A, Granath P, Crèvecoeur M, Rochaix J-D, Vener AV (2009) Phosphorylation of photosystem II controls functional macroscopic folding of photosynthetic membranes in *Arabidopsis*. Plant Cell **21:** 3950–3964

Goral TK, Johnson MP, Brain AP, Kirchhoff H, Ruban AV, Mullineaux CW (2010) Visualizing the mobility and distribution of chlorophyll proteins in higher plant thylakoid membranes: effects of photoinhibition and protein phosphorylation. Plant J **62:** 948–959

Haferkamp S, Haase W, Pascal AA, van Amerongen H, Kirchhoff H (2010) Efficient light harvesting by photosystem II requires an optimized protein packing density in grana thylakoids. J Biol Chem **285:** 17020–17028

Haferkamp S, Kirchhoff H (2008) Significance of molecular crowding in grana membranes of higher plants for light harvesting by photosystem II. Photosynth Res **95:** 129–134

Hatch MD (1987) C_4 photosynthesis: a unique blend of modified biochemistry, anatomy and ultrastructure. Biochim Biophys Acta **895:** 81–106

Herbstová M, Tietz S, Kinzel C, Turkina MV, Kirchhoff H (2012) Architectural switch in plant photosynthetic membranes induced by light stress. Proc Natl Acad Sci USA **109:** 20130–20135

Ivanov B, Asada K, Edwards GE (2007) Analysis of donors of electrons to photosystem I and cyclic electron flow by redox kinetics of P700 in chloroplasts of isolated bundle sheath strands of maize. Photosynth Res **92:** 65–74

Johnson GN (2011) Reprint of: Physiology of PSI cyclic electron transport in higher plants. Biochim Biophys Acta **1807:** 906–911

Johnson MP, Goral TK, Duffy CDP, Brain AP, Mullineaux CW, Ruban AV (2011) Photoprotective energy dissipation involves the reorganization of photosystem II light-harvesting complexes in the grana membranes of spinach chloroplasts. Plant Cell **23:** 1468–1479

Joliot P, Joliot A (1964) Etudes cinetique de la reaction photochemique liberant l'oxygene au cours de la photosynthese. C R Acad Sci Paris **258:** 4622–4625

Kirchhoff H (2008) Significance of protein crowding, order and mobility for photosynthetic membrane functions. Biochem Soc Trans **36:** 967–970

Kirchhoff H, Haase W, Wegner S, Danielsson R, Ackermann R, Albertsson P-A (2007) Low-light induced formation of semicrystalline photosystem II arrays in higher plant chloroplasts. Biochemistry **46:** 11169–11176

Kirchhoff H, Haferkamp S, Allen JF, Epstein DB, Mullineaux CW (2008) Protein diffusion and macromolecular crowding in thylakoid membranes. Plant Physiol **146:** 1571–1578

Kirchhoff H, Mukherjee U, Galla H-J (2002) Molecular architecture of the thylakoid membrane: lipid diffusion space for plastoquinone. Biochemistry **41:** 4872–4882

Kirchhoff H, Tremmel I, Haase W, Kubitscheck U (2004) Supramolecular photosystem II organization in grana thylakoid membranes: evidence for a structured arrangement. Biochemistry **43:** 9204–9213

Kouřil R, Oostergetel GT, Boekema EJ (2011) Fine structure of granal thylakoid membrane organization using cryo electron tomography. Biochim Biophys Acta **1807:** 368–374

Kramer DM, Johnson GN, Kiirats O, Edwards GE (2004) New fluorescence parameters for the determination of q(a) redox state and excitation energy fluxes. Photosynth Res **79:** 209–218

Krause GH, Weis E (1991) Chlorophyll fluorescence and photosynthesis: the basics. Annu Rev Plant Physiol Plant Mol Biol **42:** 313–349

Ku SB, Gutierrez M, Kanai R, Edwards GE (1974) Photosynthesis in mesophyll protoplasts and bundle sheath cells of various types of C_4 plants. II. Chlorophyll and Hill reaction studies. Z Pflanzenphysiol **72:** 320–337

Laemmli UK (1970) Cleavage of structural proteins during the assembly of the head of bacteriophage T4. Nature **227:** 680–685

Laetsch WM (1971) Chloroplast structural relationships in leaves of C_4 plants. *In* MD Hatch, CB Osmond, RO Slatyer, eds, Photosynthesis and Photorespiration. Wiley-Interscience, New York, pp 323–349

Lemeille S, Rochaix J-D (2010) State transitions at the crossroad of thylakoid signalling pathways. Photosynth Res **106:** 33–46

Markelz NH, Costich DE, Brutnell TP (2003) Photomorphogenic responses in maize seedling development. Plant Physiol **133:** 1578–1591

Mayne BC, Dee AM, Edwards GE (1974) Photosynthesis in mesophyll protoplasts and bundle sheath cells of various types of C_4 plants. III. Fluorescence emission spectra, delayed light emission, and P700 content. Z Pflanzenphysiol **74:** 275–291

Metha M, Sarafis V, Critchley C (1999) Thylakoid membrane architecture. Aust J Plant Physiol **26:** 709–716

Mullineaux CW (2005) Function and evolution of grana. Trends Plant Sci **10:** 521–525

Mullineaux CW (2008) Factors controlling the mobility of photosynthetic proteins. Photochem Photobiol **84:** 1310–1316

Mullineaux CW, Kirchhoff H (2007) Using fluorescence recovery after photobleaching to measure lipid diffusion in membranes. *In* AM Dopico, ed, Methods in Molecular Biology. Humana Press, Totowa, NJ, pp 267–275

Mullineaux CW, Kirchhoff H (2009) Role of lipids in the dynamics of thylakoid membranes *In* H Wada, N Murata, eds, Lipids in Photosynthesis: Essential and Regulatory Functions. Springer Science, London, pp 283–294

Mulo P, Sirpiö S, Suorsa M, Aro EM (2008) Auxiliary proteins involved in the assembly and sustenance of photosystem II. Photosynth Res **98:** 489–501

Murphy DJ (1986) The molecular organisation of the photosynthetic membranes of higher plants. Biochim Biophys Acta **864:** 33–94

Mustárdy L, Garab G (2003) Granum revisited: a three-dimensional model. Where things fall into place. Trends Plant Sci **8:** 117–122

Nevo R, Chuartzman SG, Tsabari O, Reich Z (2009) Architecture and thylakoid membrane networks. *In* H Wada, N Murata, eds, Lipids in Photosynthesis: Essential and Regulatory Functions. Springer Science, London, pp 295–328

Pesaresi P, Pribil M, Wunder T, Leister D (2011) Dynamics of reversible protein phosphorylation in thylakoids of flowering plants: the roles of STN7, STN8 and TAP38. Biochim Biophys Acta **1807:** 887–896

Pokorska B, Romanowska E (2007) Photoinhibition and D1 degradation in mesophyll and agranal bundle sheath thylakoids of maize. Funct Plant Biol **34:** 844–852

Porra RJ, Thompson WA, Kriedermann PE (1989) Determination of accurate extinction coefficient and simultaneous equations for essaying chlorophylls a and b extracted with four different solvents: verification of the concentration of chlorophyll standards by atomic absorption spectroscopy. Biochim Biophys Acta **975:** 384–394

Romanowska E, Kargul J, Powikrowska M, Finazzi G, Nield J, Drozak A, Pokorska B (2008) Structural organization of photosynthetic apparatus in agranal chloroplasts of maize. J Biol Chem **283:** 26037–26046

Sharpe R, Mahajan A, Takacs E, Stern D, Cahoon A (2011) Developmental and cell type characterization of bundle sheath and mesophyll chloroplast transcript abundance in maize. Curr Genet **57:** 89–102

Sheen J (1995) Methods for Mesophyll and Bundle Sheath Cell Separation. Academic Press, Salt Lake City, UT, pp 305–314

Staehelin LA, van der Staay GWM (1996) Structure, composition, functional organization and dynamic properties of thylakoid membranes. *In* DA Ort, CF Yocum, eds, Oxygenic Photosynthesis: The Light Reactions. Kluwer Academic Publishers, The Netherlands, pp 11–30

Svensson P, Albertsson P-A (1989) Preparation of highly enriched photosystem II vesicles by a non-detergent method. Photosynth Res **20:** 249–259

Tikkanen M, Aro E-M (2012) Thylakoid protein phosphorylation in dynamic regulation of photosystem II in higher plants. Biochim Biophys Acta **1817:** 232–238

Tremmel IG, Kirchhoff H, Weis E, Farquhar GD (2003) Dependence of plastoquinol diffusion on the shape, size, and density of integral thylakoid proteins. Biochim Biophys Acta **1607:** 97–109

Tremmel IG, Weis E, Farquhar GD (2005) The influence of protein-protein interactions on the organization of proteins within thylakoid membranes. Biophys J **88:** 2650–2660

Trissl HW, Wilhelm C (1993) Why do thylakoid membranes from higher plants form grana stacks? Trends Biochem Sci **18:** 415–419

Vladimirou E, Li M, Aldridge CP, Frigerio L, Kirkilionis M, Robinson C (2009) Diffusion of a membrane protein, Tat subunit Hcf106, is highly restricted within the chloroplast thylakoid network. FEBS Lett **583:** 3690–3696

Walters RG (2005) Towards an understanding of photosynthetic acclimation. J Exp Bot **56:** 435–447